frontiers in Microbiology

ORIGINAL RESEARCH
published: 10 December 2019
doi: 10.3389/fmicb.2019.02846

New Dihydroisocoumarin Root Growth Inhibitors From the Sponge-Derived Fungus *Aspergillus* sp. NBUF87

Liming Huang[1], Lijian Ding[1]*, Xiaohui Li[1], Ning Wang[2], Wei Cui[3], Xiao Wang[3], C. Benjamin Naman[1,4], J. Enrico H. Lazaro[5], Xiaojun Yan[1] and Shan He[1]*

[1] Li Dak Sum Yip Yio Chin Kenneth Li Marine Biopharmaceutical Research Center, College of Food and Pharmaceutical Sciences, Ningbo University, Ningbo, China, [2] Institute of Drug Discovery Technology, Ningbo University, Ningbo, China, [3] Zhejiang Provincial Key Laboratory of Pathophysiology, School of Medicine, Ningbo University, Ningbo, China, [4] Center for Marine Biotechnology and Biomedicine, Scripps Institution of Oceanography, University of California, San Diego, La Jolla, CA, United States, [5] National Institute of Molecular Biology and Biotechnology, University of the Philippines Diliman, Quezon, Philippines

OPEN ACCESS

Edited by:
László Galgóczy, Hungarian Academy of Sciences, Hungary

Reviewed by:
Yongbo Xue, Huazhong University of Science and Technology, China
Ajmal Khan, University of Nizwa, Oman
Mahmoud Fahmi Elsebai, Mansoura University, Egypt

***Correspondence:**
Lijian Ding
dinglijian@nbu.edu.cn
Shan He
heshan@nbu.edu.cn

Specialty section:
This article was submitted to Fungi and Their Interactions, a section of the journal Frontiers in Microbiology

Received: *06 September 2019*
Accepted: *25 November 2019*
Published: *10 December 2019*

Citation:
Huang L, Ding L, Li X, Wang N, Cui W, Wang X, Naman CB, Lazaro JEH, Yan X and He S (2019) New Dihydroisocoumarin Root Growth Inhibitors From the Sponge-Derived Fungus Aspergillus sp. NBUF87. Front. Microbiol. 10:2846. doi: 10.3389/fmicb.2019.02846

Six new dihydroisocoumarins, aspergimarins A–F (**1**–**6**), were discovered together with five known analogs (**7**–**11**) from a monoculture of the sponge-derived fungus *Aspergillus* sp. NBUF87. The structures of these compounds were elucidated through comprehensive spectroscopic methods, and absolute configurations were assigned after X-ray crystallography, use of the modified Mosher's method, and comparison of electronic circular dichroism (ECD) data with literature values for previously reported analogs. Compounds **1**–**11** were evaluated in a variety of bioassays, and at 100 μM, both **1** and **5** showed significant inhibitory effects on the lateral root growth of *Arabidopsis thaliana* Columbia-0 (Col-0). Moreover, at 100 μM, **5** also possessed notable inhibition against the primary root growth of Col-0. Meanwhile, **1**–**11** were all found to be inactive *in vitro* against acetylcholinesterase (AChE) (IC_{50} > 100 μM), four different types of human-derived cancer cell lines (IC_{50} > 50 μM), as well as methicillin-resistant *Staphylococcus aureus* and *Escherichia coli* (MIC > 50 μg/mL), and *Plasmodium falciparum* W2 (EC_{50} > 100 μg/mL), in phenotypic tests.

Keywords: dihydroisocoumarin, root growth inhibitor, sponge-derived fungus, *Aspergillus* sp., electronic circular dichroism

INTRODUCTION

Sponges are among the most primitive multicellular invertebrates and harbor vast microbial populations, owing largely to the unique filter-feeding physiology that is full of pores and channels (Hentschel et al., 2006; Webster and Taylor, 2012). As a result of the long-standing interaction and coevolution with sponges, marine symbiotic microorganisms have differentiated from those of terrestrial origins in terms of their biosynthetic pathways that lead to the production of structurally interesting and biologically active compounds (Thomas et al., 2010; Fan et al., 2012). Therefore, sponge-associated microbes have become an exciting area of drug discovery research (Thomas et al., 2010; Pita et al., 2016). Endophytic fungi that are associated with sponges, especially members of the genus *Aspergillus*, have been recognized as a source of structurally diverse natural products with biological activities that provide value for drug discovery (Blunt et al., 2018; Zhang et al., 2018). In the past decade, the secondary metabolites from sponge-derived *Aspergillus* fungi have been reported from many classes, including polyketides (Wang et al., 2014; Kong et al., 2015), terpenoids (Liu et al., 2009; Li D. et al., 2012), alkaloids (Zhou et al., 2013, 2014), diketopiperazines (Ahmed et al., 2017), and peptides (Lee et al., 2011). Many of these metabolites have been shown to exhibit strong antitumor, antibacterial, antiviral, and other bioactivities.

Isocoumarins and 3,4-dihydroisocoumarins, subclasses of polyketide compounds, are also lactone-containing natural products that are abundantly produced among fungi, bacteria, liverworts, lichens, as well as some higher plants (Elsebai and Ghabbour, 2016; Saeed, 2016; Hussain and Green, 2017; Chen M. et al., 2019). Moreover, these compounds have been isolated from marine sponges, insect pheromones, and venoms (Saeed, 2016). Almost 400 isocoumarins and dihydroisocoumarins have been reported to date, and these compounds have been found to be of broad interest across many pharmacological applications (Saeed, 2016; Chen M. et al., 2019). For example, isocoumarin derivatives from some marine-derived fungi are found to possess a wide range of biological properties including enzyme inhibitory (Kim et al., 2015; Chen S. et al., 2016; Wiese et al., 2016; Cai et al., 2018), cytotoxic (Wang et al., 2019; Wu et al., 2019), antibacterial (Li S. et al., 2012; Lei et al., 2017; Chen Y. et al., 2018; Wang et al., 2019), antiproliferative (Tsukada et al., 2011), anti-food allergic (Niu et al., 2018), as well as anti-inflammatory (Kim et al., 2015; Chen Y. et al., 2018; Liu et al., 2018) activities.

As part of a continuing research program investigating the biologically active secondary metabolites from sponge-derived fungi (Ding et al., 2018; Huang et al., 2019; Li W. et al., 2019), a detailed chemical investigation was initiated on the culture of fungus *Aspergillus* sp. NBUF87. The fungus was isolated from a South China Sea marine sponge of the genus *Hymeniacidon*. The EtOAc extract of the culture of fungus *Aspergillus* sp. NBUF87 exhibited inhibitory effects on the root growth of *Arabidopsis thaliana* Columbia-0 (Col-0), a typical model organism for studying plant growth and development. The separation and purification of the bioactive extract led to the discovery of six new dihydroisocoumarin compounds (**1**−**6**) and five known analogs (**7**−**11**) (**Figure 1**). Herein, the detailed isolation and structure elucidation of these dihydroisocoumarin derivatives, together with the evaluation of their inhibitory effects against the root growth of Col-0 and a preliminary broader biological activity screening are described.

MATERIALS AND METHODS

General Experimental Procedures

Optical rotation measurements were conducted with a JASCO P-2000 digital polarimeter. IR and UV spectra were obtained with a Thermo Scientific Nicolet iS5 FT-IR spectrometer and a Thermo Scientific Evolution 201 spectrophotometer, respectively. Electronic circular dichroism (ECD) spectra were collected on a JASCO J-1500 spectrophotometer. 1D and 2D NMR spectra were recorded in DMSO-d_6 (or $CDCl_3$) with a Palo Alto Varian 600 MHz spectrometer, using standard pulse sequences. HRESIMS data were collected on an Agilent Technologies 6224 TOF MS. X-ray single-crystal diffraction data were acquired using an Agilent Gemini Ultra diffractometer with Cu Kα radiation (λ = 1.54178 Å). Medium-pressure liquid chromatography (MPLC) was performed using a Bonna-Agela FLEXA purification instrument. Column chromatography (CC) was carried out with silica gel (200−300 mesh, Qingdao) and Amersham Biosciences Sephadex LH-20. Reversed-phase HPLC (RP-HPLC) was conducted using a Waters 1525 binary HPLC pump equipped with a Waters 2996 photodiode array detector and a YMC-Pack C18 column (YMC, 20 × 250 mm, 5 μm).

Fungal Material

The fungus *Aspergillus* sp. NBUF87 was isolated from the sponge *Hymeniacidon* sp. obtained from the Paracel Islands in the South China Sea, and was determined as being *Aspergillus* sp. by its morphology and gene sequence (ITS rDNA region) analyses (GenBank accession no. MH595747.1). The strain specimen was deposited in PDB medium to the repository conserved at the College of Food and Pharmaceutical Sciences, Ningbo University, China.

Fermentation, Extraction, and Isolation

Spores of *Aspergillus* sp. NBUF87 were initially inoculated into Erlenmeyer flasks (1 L) containing 400 mL of the seed medium (potato dextrose broth powder 26 g/L and sea salt 35 g/L dissolved in distilled water) and were grown on a shaker (150 r/min) for 100 h at 28°C. The subsequent amplified fermentation was conducted in 105 × 1 L Erlenmeyer flasks, each containing solid rice medium (rice 120 g, sea salt 6.3 g, purified H_2O 180 mL), followed by inoculation with 30 mL of the seed culture. After fermentation at room temperature under static conditions for 6 weeks, the fermented substrate was repeatedly extracted with EtOAc. Removal of EtOAc under reduced pressure yielded 54 g of crude extract, which was subjected to vacuum liquid chromatography (VLC) on silica gel column eluting with a petroleum ether/EtOAc stepwise gradient system (from 1:0 to 0:1) to generate seven fractions (Fr. 1−7).

Fraction 4 (3.9 g) was subjected to Sephadex LH-20 gel filtration chromatography, eluted with isocratic CH_2Cl_2-CH_3OH (1:1, v/v) to furnish five sub-fractions (Fr. 4A−4F). The further separation of Fr. 4E (1.8 g) was conducted by reversed-phase ODS MPLC with a gradient elution of CH_3OH/H_2O (from 25 to 100% CH_3OH, flow rate 20 mL/min, 180 min, UV detection at 210 nm) to afford 60 test tube sub-fractions. Subsequently, aspergimarin A (**1**, 15.3 mg, t_R 33.4 min) was purified from Fr. 4E-20 by semi-preparative RP-HPLC [YMC-Pack C18 column (YMC, 20 × 250 mm, 5 μm), UV detection at 210 and 246 nm] with 28% CH_3CN/H_2O at 2 mL/min. Aspergimarin E (**5**, 3.6 mg, t_R 40.2 min), compounds **10** (4.3 mg, t_R 72.3 min) and **11** (4.7 mg, t_R 58.2 min) were purified from Fr. 4E-19 by semi-preparative RP-HPLC with 24% CH_3CN/H_2O at 2 mL/min. Aspergimarin F (**6**, 3.4 mg, t_R 57.3 min) was purified from Fr. 4E-18 by semi-preparative RP-HPLC with 24% CH_3CN/H_2O at 2 mL/min. Fr. 4B (1.0 g) was conducted by MPLC (30−90% CH_3OH/H_2O, flow rate 20 mL/min, 120 min, UV detection at 210 nm) to produce 10

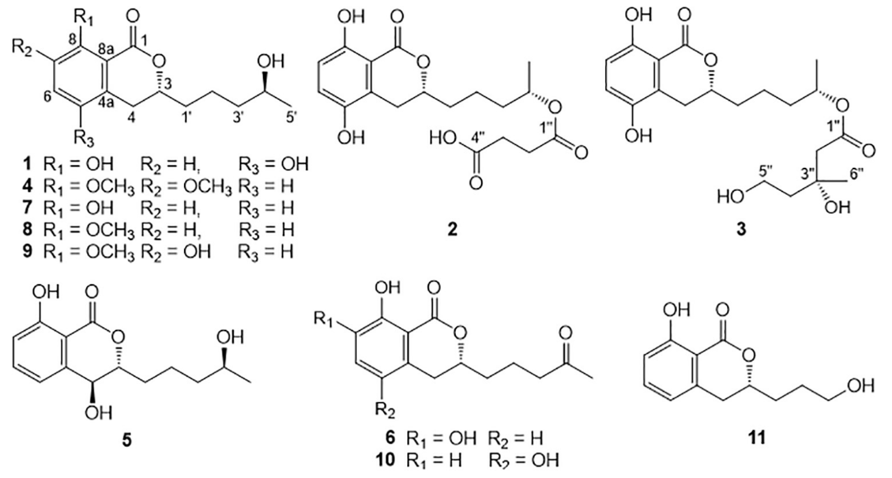

FIGURE 1 | Structures of isolated dihydroisocoumarin derivatives (**1**–**11**).

sub-fractions (Fr. 4B-1−4B-10). Fr. 4B-4 was further purified by semi-preparative RP-HPLC with 42% CH_3OH/H_2O at 2 mL/min to yield compound **9** (43.1 mg, t_R 45.0 min). Fr. 4B-8 was further purified by semi-preparative RP-HPLC with 60% CH_3OH/H_2O at 2 mL/min to afford compound **7** (56.0 mg, t_R 26.7 min) (**Supplementary Figures S1–S10, S41–S60**).

Fraction 5 (4.8 g) was separated by Sephadex LH-20 gel filtration chromatography utilizing an isocratic elution gradient of CH_2Cl_2−CH_3OH (1:1, v/v) to afford three sub-fractions (Fr. 5A−5C). The further separation of Fr. 5B (2.5 g) was conducted by RP-MPLC (ODS, 15−100% CH_3OH/H_2O, flow rate 20 mL/min, 140 min, UV detection at 210 nm) to give 35 tubes. Aspergimarin B (**2**, 2.5 mg, t_R 31.4 min) and aspergimarin C (**3**, 3.8 mg, t_R 22.9 min) were further purified from Fr.5B-23 by semi-preparative RP-HPLC with 30% CH_3CN/H_2O at 4 mL/min. Fr. 5A (0.9 g) was separated by MPLC (ODS, 25−100% CH_3OH/H_2O, flow rate 20 mL/min, 150 min, UV detection at 210 nm) to obtain 38 tubes. Fr.5A-15 was further purified by semi-preparative RP-HPLC with 25% CH_3CN/H_2O at 4 mL/min to afford aspergimarin D (**4**, 6.3 mg, t_R 31.0 min). Fr. 5A-14 was purified by semi-preparative RP-HPLC with 22% CH_3CN/H_2O at 4 mL/min to afford compound **8** (26.1 mg, t_R 31.6 min) (**Supplementary Figures S11–S40**).

*Aspergimarin A (**1**):* white, crystals; mp 177.9−178.8 ℃; [α]20 D −34.0 (*c* 0.2, $CHCl_3$); UV (MeOH) λ_{max} (log ε): 219 (4.14), 248 (3.77), 346 (3.58) nm; CD (*c* = 0.68 mM, MeOH) λ_{max} (Δε): 223 (+ 2.15), 237 (−1.93), 245 (−1.10), 259 (−6.32) nm; IR (KBr) ν_{max}: 3205, 1647, 1588, 1483, 1354, 1281, 820, 795, 700 cm^{-1}; ^1H and ^{13}C NMR data, see **Table 1**; HRESIMS *m/z* 265.1082 [M − H]$^-$ (calcd for $C_{14}H_{17}O_5$, 265.1081).

*Aspergimarin B (**2**):* brown, oil; [α]24 D −10.6 (*c* 0.2, MeOH); UV (MeOH) λ_{max} (log ε): 211 (4.24), 345 (3.66) nm; CD (*c* = 0.33 mM, MeOH) λ_{max} (Δε): 225 (+ 0.88), 235 (−1.54), 243 (−0.81), 257 (−5.77) nm; IR (KBr) ν_{max}: 3226, 2929, 1723, 1675, 1469, 1379, 1207, 829 cm^{-1}; ^1H and ^{13}C NMR data, see **Table 1**; HRESIMS *m/z* 365.1232 [M − H]$^-$ (calcd for $C_{18}H_{21}O_8$, 365.1242).

*Aspergimarin C (**3**):* brown, oil; [α]24 D −10.8 (*c* 0.3, MeOH); UV (MeOH) λ_{max} (log ε): 219 (4.27), 344 (3.63) nm; CD (*c* = 0.45 mM, MeOH) λ_{max} (Δε): 229 (+ 0.86), 238 (−1.44), 243 (−0.32), 257 (−5.37) nm; IR (KBr) ν_{max}: 3368, 2921, 1671, 1469, 1378, 1287, 1206, 1123 cm^{-1}; ^1H and ^{13}C NMR data, see **Table 1**; HRESIMS *m/z* 435.1416 [M + K]$^+$ (calcd for $C_{20}H_{28}KO_8$, 435.1415).

*Aspergimarin D (**4**):* yellow, oil; [α]24 D −82.2 (*c* 0.5, MeOH); UV (MeOH) λ_{max} (log ε): 214 (4.16), 312 (3.24) nm; CD (*c* = 0.68 mM, MeOH) λ_{max} (Δε): 221 (−6.98), 241 (−0.28), 256 (−2.47), 284 (−0.48), 311 (−1.61) nm; IR (KBr) ν_{max}: 3402, 2935, 1717, 1489, 1455, 1418, 1259, 1131, 1052, 963 cm^{-1}; ^1H and ^{13}C NMR data, see **Table 2**; HRESIMS *m/z* 295.1537 [M + H]$^+$ (calcd for $C_{16}H_{23}O_5$, 295.1540).

*Aspergimarin E (**5**):* colorless, oil; [α]24 D + 17.7 (*c* 0.3, MeOH); UV (MeOH) λ_{max} (log ε): 209 (4.17), 246 (3.52), 312 (3.42) nm; CD (*c* = 0.56 mM, MeOH) λ_{max} (Δε): 206 (−8.37), 218 (−0.47), 224 (−1.04), 243 (+ 3.53), 264 (−0.71), 280 (−0.01), 311 (−0.53) nm; IR (KBr) ν_{max}: 3367, 2920, 1672, 1461, 1230, 1117, 823 cm^{-1}; ^1H and ^{13}C NMR data, see **Table 2**; HRESIMS *m/z* 289.1034 [M + Na]$^+$ (calcd for $C_{14}H_{18}NaO_5$, 289.1046).

*Aspergimarin F (**6**):* yellow, amorphous powder; [α]24 D −7.5 (*c* 0.2, MeOH); UV (MeOH) λ_{max} (log ε): 221 (4.14), 256 (3.71), 332 (3.44) nm; CD (*c* = 0.57 mM, MeOH) λ_{max} (Δε): 208 (−8.75), 240 (+ 2.67), 266 (−1.47) nm; IR (KBr) ν_{max}: 3360, 2920, 2849, 2361, 1707, 1664, 1452, 1272, 1135, 668 cm^{-1}; ^1H and ^{13}C NMR data, see **Table 2**; HRESIMS *m/z* 287.0879 [M + Na]$^+$ (calcd for $C_{14}H_{16}NaO_5$, 287.0890).

X-Ray Crystal Structure Analysis of 1

A single crystal of **1** was obtained from 90% CH_3OH/H_2O. Crystal X-ray diffraction data was collected on an Agilent Gemini Ultra diffractometer with Cu Kα radiation (λ = 1.54178 Å). The structure was solved by direct methods (SHELXS−97) and refined with full-matrix least-squares difference Fourier techniques. All non-hydrogen atoms were refined anisotropically,

TABLE 1 | ^{1}H (600 MHz) and ^{13}C (150 MHz) NMR data of **1**–**3** collected in DMSO-d_6.

Position	1		2		3	
	δ_H (*J* in Hz)	δ_C, type	δ_H (*J* in Hz)	δ_C, type	δ_H (*J* in Hz)	δ_C, type
1		169.5, C		169.5, C		169.5, C
3	4.59, m	79.4, CH	4.59, m	79.2, CH	4.59, m	79.2, CH
4	3.06, dd (16.9, 3.4) 2.60, dd (16.9, 11.6)	26.3, CH_2	3.05, dd (16.9, 3.3) 2.60, dd (16.9, 11.5)	26.4, CH_2	3.05, dd (16.9, 3.4) 2.60, dd (16.9, 11.5)	26.3, CH_2
4a		124.5, C		124.0, C		124.5, C
5		146.6, C		145.7, C		145.6, C
6	7.07, d (8.9)	123.9, CH	7.06, d (8.9)	124.0, CH	7.06, d (8.9)	123.9, CH
7	6.72, d (8.9)	115.1, CH	6.72, d (8.9)	115.2, CH	6.72, d (8.9)	115.2, CH
8		153.9, C		153.9, C		153.9, C
8a		108.2, C		108.3, C		108.2, C
1′	1.78, m 1.68, m	34.3, CH_2	1.76, m 1.70, m	33.9, CH_2	1.74, m	33.9, CH_2
2′	1.46, m	20.8, CH_2	1.44, m	20.3, CH_2	1.46, m	20.3, CH_2
3′	1.36, m	38.6, CH_2	1.55, m	34.9, CH_2	1.55, m	34.9, CH_2
4′	3.60, m	65.6, CH	4.83, m	70.2, CH	4.83, m	69.8, CH
5′	1.05, d (6.2)	23.7, CH_3	1.16, d (6.3)	19.8, CH_3	1.17, d (6.2)	19.8, CH_3
1′′				171.8, C		170.4, C
2′′			2.45, m 1.24, m	28.9, CH_2	2.38, m	46.9, CH_2
3′′			2.46, m	29.1, CH_2		69.8, C
4′′				173.5, C	1.67, m	43.7, CH_2
5′′					3.54, m	57.2, CH_2
6′′					1.18, s	27.4, CH_3
8-OH	10.38, s		10.37, s		10.37, s	
3′′-OH					4.53, s	
5′′-OH					4.36, s	

s, singlet; d, doublet; dd, doublet of doublets; m, multiplet.

and hydrogen atoms were placed in the idealized geometrical positions and refined isotropically with a riding model. Crystallographic data for **1** have been deposited in the Cambridge Crystallographic Data Center as supplementary publication no. CCDC 1919904. Copies of the data can be obtained, free of charge, on application to the Director, CCDC, 12 Union Road, Cambridge CB21EZ, United Kingdom (fax: + 44-(0)1223-336033, or e-mail: deposit@ccdc.cam.ac.uk).

*Crystal data of aspergimarin A (**1**):* $C_{14}H_{18}O_5$, M_R = 266.28, monoclinic, a = 4.9195(3) Å, b = 24.7434(17) Å, c = 5.6478(4) Å, $\alpha = \gamma = 90°$, β = 101.812(2)°, V = 672.92(8) Å^3, space group $P2_1$, Z = 2, D_c = 1.314 mg/m^3, μ = 0.829 mm^{-1}, and F(000) = 284. Crystal size: 0.200 × 0.170 × 0.130 mm^3. Independent reflections: 2294 (R_{int} = 0.0377). Final R indices [I > 2 sigma (I)], R_1 = 0.0717, wR_2 = 0.2076. Goodness of fit on F^2 was 1.109.

Preparation of MTPA Esters of 3–5 for Modified Mosher's Analysis

Under an atmosphere of nitrogen, pyridine-d_5 (500 μL) and (R)-MTPA-Cl (8 μL) was sequentially added to an EP tube containing compounds **3**, **4**, or **5** (1.0 mg), separately. The mixture was shaken at 28 ℃ for 12 h and then purified by RP-HPLC to obtain the (S)-MTPA esters **3a**, **4a**, and **5a**. By the same procedure, the (R)-MTPA esters **3b**, **4b**, and **5b** were obtained using (S)-MTPA-Cl as a reagent. Key ^{1}H NMR signals used for configurational assignments were determined by respective ^{1}H–^{1}H COSY correlations and the already completed full assignments of ^{1}H NMR data for **3**, **4**, and **5** (see **Supplementary Figures S61–S72**).

The C-3′′ absolute configuration of **3** were established as R on the basis of the $\Delta\delta$ values ($\Delta\delta_{H-2''}$: −0.01; $\Delta\delta_{H-4''}$: + 0.03; $\Delta\delta_{H-5''}$: + 0.01) of the (S)- and (R)-MTPA esters (**3a** and **3b**). **3a**: H-2′′ (δ_H 2.37), H-4′′ (δ_H 1.89), H-5′′ (δ_H 4.45); **3b**: H-2′′ (δ_H 2.38), H-4′′ (δ_H 1.86), H-5′′ (δ_H 4.44).

The C-4′ absolute configuration of **4** was established as S on the basis of the $\Delta\delta$ values ($\Delta\delta_{H-3'}$: + 0.05, + 0.05; $\Delta\delta_{H-5'}$: −0.10) of the (S)- and (R)-MTPA esters (**4a** and **4b**). **4a**: H-3′ (δ_H 1.64, 1.27), H-5′ (δ_H 1.21); **4b**: H-3′ (δ_H 1.59, 1.22), H-5′ (δ_H 1.31).

Both C-4 and C-4′ absolute configuration of **5** were established as S on the basis of the $\Delta\delta$ values ($\Delta\delta_{H-3}$: + 0.17; $\Delta\delta_{H-5}$: −0.19; $\Delta\delta_{H-6}$: −0.02; $\Delta\delta_{H-1'}$: + 0.08, + 0.13; $\Delta\delta_{H-2'}$: + 0.03; $\Delta\delta_{H-3'}$: + 0.07, + 0.08; $\Delta\delta_{H-5'}$: −0.07) of the (S)- and (R)-MTPA esters (**5a** and **5b**). **5a**: H-3 (δ_H 4.65), H-5 (δ_H 7.27), H-6 (δ_H 7.63), H-1′ (δ_H 1.66, 1.53), H-2′ (δ_H 1.49), H-3′ (δ_H 1.60, 1.32), H-5′ (δ_H 1.25); **5b**: H-3 (δ_H 4.48), H-5 (δ_H 7.46), H-6 (δ_H 7.65), H-1′ (δ_H 1.58, 1.40), H-2′ (δ_H 1.46), H-3′ (δ_H 1.53, 1.24), H-5′ (δ_H 1.32).

TABLE 2 | ^{1}H (600 MHz) and ^{13}C (150 MHz) NMR data of **4–6**.

Position	4 (DMSO-d_6)		5 ($CDCl_3$)		6 (DMSO-d_6)	
	δ_H (*J* in Hz)	δ_C, type	δ_H (*J* in Hz)	δ_C, type	δ_H (*J* in Hz)	δ_C, type
1		161.5, C		168.7, C		169.8, C
3	4.37, m	78.1, CH	4.47, m	83.6, CH	4.61, m	79.9, CH
4	2.91, dd (16.1, 3.1) 2.76, dd (16.1, 11.2)	32.7, CH_2	4.71, d (7.5)	67.5, CH	2.91, dd (16.2, 3.3) 2.80, dd (16.2, 11.4)	31.4, CH_2
4a		132.3, C		141.7, C		129.3, C
5	7.06, d (8.3)	122.7, CH	7.03, d (7.4)	116.3, CH	6.63, d (8.0)	117.5, CH
6	7.28, d (8.3)	117.7, CH	7.54, t (8.4, 7.4)	137.0, CH	7.00, d (8.0)	121.6, CH
7		152.2, C	6.69, d (8.4)	117.9, CH		144.4, C
8		150.1, C		162.1, C		150.0, C
8a		119.0, C		106.8, C		108.4, C
1′	1.70, m 1.60, m	34.1, CH_2	1.87, m 1.82, m	31.5, CH_2	1.71, m 1.63, m	33.3, CH_2
2′	1.44, m	20.9, CH_2	1.71, m 1.63, m	21.0, CH_2	1.65, m 1.57, m	18.7, CH_2
3′	1.34, m	38.7, CH_2	1.51, m	38.7, CH_2	2.51, t (6.2)	42.1, CH_2
4′	3.59, m	65.7, CH	3.85, m	67.9, CH		208.2, C
5′	1.04, d (6.1)	23.7, CH_3	1.21, d (6.2)	23.9, CH_3	2.08, s	29.8, CH_3
7-OCH_3	3.81, s	56.1, CH_3				
8-OCH_3	3.75, s	60.7, CH_3				
8-OH			10.97, s			

s, singlet; d, doublet; dd, doublet of doublets; t, triplet; m, multiplet.

Plant Growth Response Assays

Arabidopsis thaliana Col-0, a model organism for plant growth and development, was used to test each isolated compound according to a previously described protocol (Li X. et al., 2018; Huang et al., 2019). Plants grown in 2% (*v/v*) DMSO were used as the negative control. Seeds of Col-0 incubated in 1 μM of 6-benzylaminopurine (BAP) were selected as the positive control. Test samples were dissolved in 2% (*v/v*) DMSO at various test concentrations for the experiment.

In vitro AChE Activity Assays

For compounds **1−11**, the *in vitro* acetylcholinesterase (AChE) activity was assessed by the colorimetric method in 96-well plates according to a previously reported method (Santos et al., 2012). Donepezil was selected as the positive control with IC_{50} value of 11.9 nM (Chen H. et al., 2018).

In vitro Cancer Cell Cytotoxicity Assays

The *in vitro* cytotoxic activities of all isolated compounds against four human cancer cell lines (CCRF-CEM, MDA-MB-231, HCT-116, and AGS) were evaluated by the MTT method as previously described (Huang et al., 2019; Li W. et al., 2019). 7-Ethyl-10-hydroxycamptothecin (1.3, 10.8, 9.9, and 4.2 nM, respectively) was used as the positive control against four above-mentioned human cancer cell lines.

Antibacterial Activity Assays

Compounds **1−11** were evaluated for their antibacterial activities against methicillin-resistant *Staphylococcus aureus* ATCC43300 and *Escherichia coli* ATCC25922 in 96-well plates according to the method described by Gu et al. (2018). Ciprofloxacin was selected as a positive control against the above-mentioned bacteria with MIC values of 0.5 μg/mL.

In vitro Antimalarial Activity Assays

The *in vitro* antimalarial activity of the compounds was evaluated against the parasite (*Plasmodium falciparum* W2), which was cultured continuously according to a previously described method (Lazaro et al., 2006). Chloroquine, atovaquone, and artemisinin were used as positive controls against the above parasite with EC_{50} values of 112, 2.5, and 160 nM, respectively.

RESULTS AND DISCUSSION

Structure Elucidation

Compound **1** was isolated as white crystals. The molecular formula of **1** was determined to be $C_{14}H_{18}O_5$ based on an ion peak observed in HRESIMS spectrum (*m/z* $[M - H]^-$ 265.1082, calcd for $C_{14}H_{17}O_5$, 265.1081), and this implied the compound has six degrees of unsaturation. The ^{1}H NMR data of **1** (**Table 1**) demonstrated two aromatic signals [(δ_H 7.07, d, *J* = 8.9 Hz, H-6) and (δ_H 6.72, d, *J* = 8.9 Hz, H-7)] that were suggestive of two *ortho* protons. In addition, one phenolic hydroxy group at δ_H 10.38 (1H, s, 8-OH), two oxygenated methine groups at δ_H 4.59 (1H, m, H-3) and 3.60 (1H, m, H-4′), four methylene groups at δ_H 3.06 (1H, dd, H-4α), 2.60 (1H, dd, H-4β), 1.78 (1H, m, H-1′α), 1.68 (1H, m, H-1′β), 1.46 (2H, m, H-2′), and 1.36 (2H, m, H-3′), and one methyl group at δ_H 1.05 (3H, d, H-5′) were observed in the ^{1}H NMR spectrum of **1**. The ^{13}C NMR and DEPT spectra together for **1** indicated 14 carbon signals (**Table 1**), including a carbonyl at δ_C 169.5 (C-1), six aromatics at δ_C 153.9 (C-8), 146.6 (C-5), 124.5 (C-4a), 123.9 (C-6), 115.1 (C-7), and 108.2 (C-8a), and seven alkyl carbons that were two oxygenated methines at δ_C 79.4 (C-3) and 65.6 (C-4′), four hydrocarbon methylenes at δ_C 38.6 (C-3′), 34.3 (C-1′), 26.3 (C-4), and 20.8 (C-2′), and a methyl at δ_C 23.7 (C-5′). In total, the NMR data suggested the presence of a dihydroisocoumarin skeleton contained in **1**. The $^1H-^1H$ COSY correlations of H-5′/H-4′/H-3′/H-2′/H-1′ further indicated a continuous spin system in the molecule, identified as -CH_2-CH_2-CH_2-CH(OH)-CH_3 (**Figure 2**). Furthermore, according to the key HMBC correlations presented in **Figure 2**, including from H-2′ to C-3, from H-4 to C-1′, C-3, C-5, C-4a, and C-8a, as well as from 8-OH to C-7, C-8, and C-8a, the planar structure of **1** was established as shown. Finally, on the basis of X-ray single-crystal diffraction analysis (**Figure 3**), the absolute configuration of **1** was established as 3*R*,4′*S*, and this new molecule was given the trivial name aspergimarin A.

Compound **2** was obtained as a brown oil, and the molecular formula of $C_{18}H_{22}O_8$ was assigned to this molecule by the anion HRESIMS peak at *m/z* 365.1232 $[M - H]^-$ (calcd for $C_{18}H_{21}O_8$, 365.1242). The ^1H and ^{13}C NMR spectroscopic data of **2** (**Table 1**) resembled those of **1**, and it was determined that the core structure of an oxygenated hydrocarbon-extended dihydroisocoumarin was shared between these molecules. The $^1H-^1H$ COSY correlation between H-2′′ and H-3′′, along with key HMBC correlations from H-3′′ (δ_H 2.46) to C-1′′ (δ_C 171.8) and C-4′′ (δ_C 173.5) (**Figure 2**), indicated the existence of the linear chain -OCO-CH_2-CH_2-CO_2H in the structure of **2**. Furthermore, according to the same biosynthetic pathway with **1** based on and the key HMBC correlation observed from H-4′ (δ_H 4.83) to C-1′′, the planar structure of **2** was established. The absolute configuration for **2** was suggested as being 3*R*,4′*S* based on the biosynthetic logic that it would match that of **1**. The CD spectra of **1** and **2** (**Figure 4**) are able to be overlapped, with the same Cotton effects observed, which further support the configurational assignment. Accordingly, the resolved structure of compound **2** was afforded the trivial name aspergimarin B.

Compound **3** was also obtained as a brown oil, and its molecular formula of $C_{20}H_{28}O_8$ was determined by the potassium cation adduct peak in the HRESIMS spectrum at *m/z* 435.1416 $[M + K]^+$ (calcd for $C_{20}H_{28}KO_8$, 435.1416). The CD spectrum of **3** (**Figure 4**) and the ^1H and ^{13}C NMR spectroscopic data (**Table 1**) were similar to those of both **1** and **2**, indicating

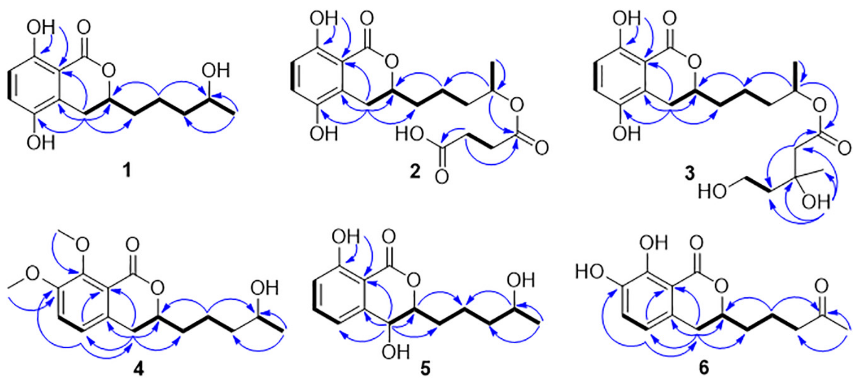

FIGURE 2 | $^1H-^1H$ COSY and key HMBC correlations observed for **1**–**6**.

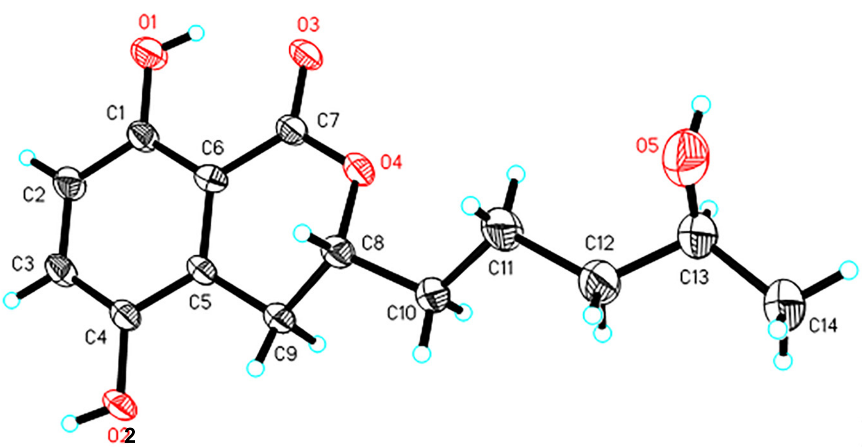

FIGURE 3 | X-ray ORTEP drawing of **1**.

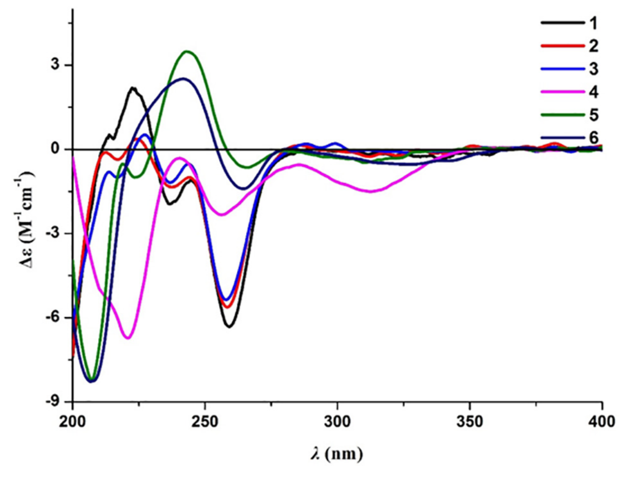

FIGURE 4 | Experimental ECD spectra of **1**–**6**, collected in MeOH.

that this molecule is another oxygenated hydrocarbon-extended dihydroisocoumarin analog with the same absolute configuration at C-3 and C-4′. It was determined from a ^{1}H−^{1}H COSY correlation of H-4′′/H-5′′ and the key HMBC correlations from H-2′′ (δ_H 2.38) to C-1′′ (δ_C 170.4) and C-4′′ (δ_C 43.7), as well as from 3′′-OH (δ_H 4.53) to C-2′′ (δ_C 46.9), C-3′′ (δ_C 69.8) and C-6′′ (δ_C 27.4) (**Figure 2**), that there is a different secondary carbon side chain [-OCO-CH_2-C(CH_3)(OH)-CH_2-CH_2OH] in the molecule of **3** as compared to **2**. Furthermore, the key HMBC correlation observed from H-4′ (δ_H 4.83) to C-1′′ allowed for the planar structure of **3** to be completed. Since the biosynthetic logic of **3** with relation to **1** and **2**, together with the matching CD data of these molecules allowed the partial absolute configuration to be assigned as 3*R*,4′*S*, only one stereocenter remained uncertain. Using the modified Mosher's method (**Figure 5**) (Gu et al., 2018) the absolute configuration of C-3′′ of **3** was established as being *R*. Therefore, the absolute configuration of **3** was determined to be 3*R*,4′*S*,3′′*R*.

Compound **4** was obtained as a yellow oil, and the molecular formula of this molecule was determined to be $C_{16}H_{22}O_5$ was based on a peak observed in the HRESIMS spectrum at *m/z* 295.1537 [M + H]$^+$ (calcd for $C_{16}H_{23}O_5$, 295.1540). The data of **4** from spectroscopic analysis, including UV, IR, and NMR, were extremely similar to those reported for the known compound, penicimarin C (**9**) (Qi et al., 2013). The exceptions noted were determined to be due to the substitution of one methoxy group for a proton at C-7. The placement of the additional methoxy group at C-7 was determined from key HMBC correlations observed from H-5 (δ_H 7.06) to C-4 (δ_C 32.7), C-7 (δ_C 152.2), and C-8a (δ_C 119.0), and from 7-*O*-CH_3 (δ_H 3.81) to C-7, together with the ^{1}H−^{1}H COSY correlation of H-5/H-6 (δ_H 7.28) (**Figure 2**). Accordingly, the planar structure of **4** was unambiguously established as shown. Compared to the CD data of **1** and some previously described values for dihydroisocoumarins (Choukchou-Braham et al., 1994), the observed CD spectrum of **4** (**Figure 4**) indicated the *R* configuration at C-3. The absolute configuration at the side chain was suggested as 4′*S* to match that of **1** according to biosynthetic logic, and this was confirmed by use of the modified Mosher's method (**Figure 5**). Thus, the absolute configuration of **4** was determined to be 3*R*,4′*S*.

Compound **5** was isolated as a colorless oil, and its molecular formula was established as being $C_{14}H_{18}O_5$ according to the associated sodiated molecular ion peak in the HRESIMS spectrum at *m/z* 289.1034 [M + Na]$^+$ (calcd for $C_{14}H_{18}NaO_5$, 289.1046). This formula for **5** corresponds to an additional OH with respect to **1**, and the ^{1}H and ^{13}C NMR data (**Table 2**) suggested shared carbon skeletons with the substitution of an additional hydroxy group. From the chemical shift differences calculated between **5** and **1**, the additional hydroxy group of **5** was suggested to be at C-4. This assignment was further supported by key HMBC correlations from H-4 (δ_H 4.71) to C-5 (δ_C 116.3) and from H-5 (δ_H 7.03) to C-4 (δ_C 67.5), together with the ^{1}H−^{1}H COSY correlation of H-4/H-3 (δ_H 4.47) (**Figure 2**). The absolute configuration at C-3 was determined to be *R* by the comparison of CD data with **1** and **4** (**Figure 4**). The absolute configuration of chiral centers at both C-4 and C-4′ in **5** was established as being *S* by use of the modified Mosher's method (**Figure 5**). Therefore, the absolute configuration of **5** was determined to be 3*R*,4*S*,4′*S*.

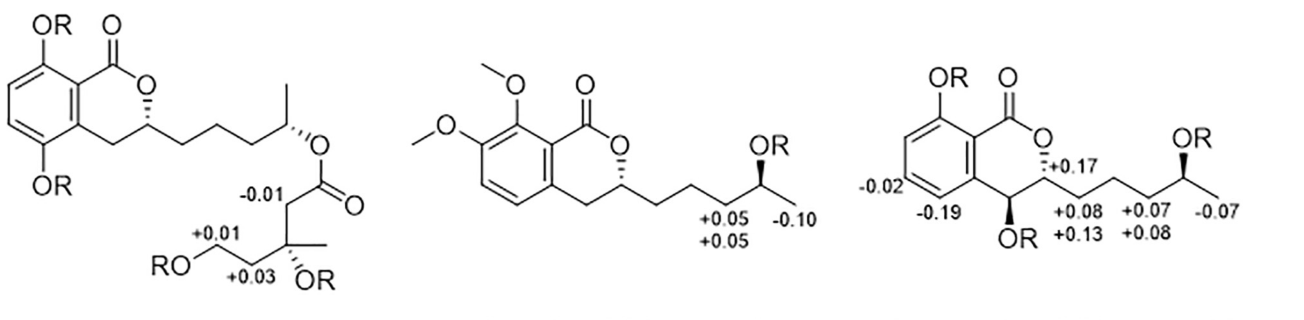

3a: R = (*S*)-MTPA ester of **3**
3b: R = (*R*)-MTPA ester of **3**
4a: R = (*S*)-MTPA ester of **4**
4b: R = (*R*)-MTPA ester of **4**
5a: R = (*S*)-MTPA ester of **5**
5b: R = (*R*)-MTPA ester of **5**

FIGURE 5 | Modified Mosher's analysis for **3**–**5**. Values shown denote $\Delta\delta$ ($\delta_S - \delta_R$) (ppm) for the MTPA esters of **3**–**5**.

Compound **6** was isolated as a yellow amorphous powder, and its molecular formula was determined to be $C_{14}H_{16}O_5$ by an associated sodiated molecular ion peak in the HRESIMS spectrum at *m/z* 287.0879 $[M + Na]^+$ (calcd for $C_{14}H_{16}NaO_5{}^+$, 287.0890). The spectroscopic data of **6**, including UV, IR, and NMR, resembled those previously reported for the known molecule penicilloxalone B (**10**) (Ren et al., 2019). From the ^{1}H and ^{13}C NMR data, it was obvious that the aromatic substitution patterns of **6** and **10** differed, with **6** bearing protons at C-5 and C-6 while **10** has protons at C-6 and C-7. Furthermore, the key HMBC correlations observed from H-5 (δ_H 6.63) to C-4 (δ_C 31.4), C-7 (δ_C 144.4), and C-8a (δ_C 108.4) together with the ^{1}H−^{1}H COSY correlation of H-5/H-6 (δ_H 7.00) (**Figure 2**) corroborated that the two phenolic hydroxy groups of **6** were situated at C-7 and C-8 (δ_C 150.0). The absolute configuration of **6** was determined to be 3*R*, the same as for **10**, by comparison of the observed CD spectrum for this molecule with reported data for **10** (**Figure 4**).

Five additional compounds isolated from *Aspergillus* sp. NBUF87 in the course of this study were determined, by comparison of the spectroscopic and spectrometric data of each with reported values, to be the known isocoumarin derivatives aspergillumarin B (**7**) (Li S. et al., 2012), penicimarin B (**8**) (Qi et al., 2013), penicimarin C (**9**) (Qi et al., 2013), penicilloxalone B (**10**) (Ren et al., 2019), and (*R*)-3-(3-hydroxypropyl)-8-hydroxy-3,4-dihydroisocoumarin (**11**) (Sun et al., 2017). The absolute configurations for **7**-**9** were established to be 3*R*, 4′*S* because the CD spectra (see **Supplementary Figures S61, S73**), and optical rotation data matched literature values (Li S. et al., 2012; Qi et al., 2013). The absolute configuration of **10** and **11** was also determined to be 3*R* because the optical rotation data matched literature reported values for these molecules (Sun et al., 2017; Ren et al., 2019).

Effects of Compounds 1−11 on Plant Growth of *Arabidopsis thaliana* Columbia-0

The isolated compounds **1**−**11** were subjected to bioassays for testing plant growth response using *A. thaliana* Col-0, a model plant growth organism. At 100 μM, for both **1** and **5,** root growth inhibitory activity was observed against Col-0. Interestingly, while **1** showed only significant inhibitory effect on the lateral root growth of Col-0, **5** caused notable inhibition of both lateral root and primary root growth, as shown in **Figure 6**. Compounds **2**-**4** and **6**-**11** did not show any obvious activity in the same plant growth response assay at 100 μM.

Results of Compounds 1−11 Against Four Additional Bioassays

All compounds isolated in this study (**1**−**11**) were also tested for their *in vitro* inhibitory activity of AChE in a biochemical assay, and phenotypic tests for cytotoxicity against four human-derived cancer cell lines, namely, CCRF-CEM (acute lymphoblastic leukemia T lymphocyte), MDA-MB-231 (breast cancer), HCT-116 (colon cancer), and AGS (gastric adenocarcinoma), and antibacterial activity toward methicillin-resistant *S. aureus* ATCC43300 and *E. coli* ATCC25922, and antimalarial activity against *P. falciparum* W2. None of these compounds exhibited inhibition of AChE (IC_{50} > 100 μM), cytotoxic activities against any of the cell lines tested (IC_{50} > 50 μM), antibacterial activities toward the two bacteria (MIC > 50 μg/mL), or antimalarial activity against the parasite (EC_{50} > 100 μg/mL).

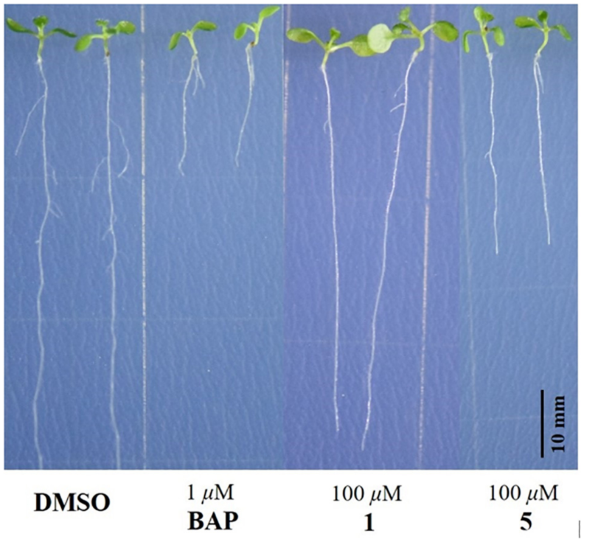

FIGURE 6 | Responses of 100 μM addition of **1** and **5** on the root growth of *Arabidopsis thaliana* Columbia-0 at 10 days after seed germination. DMSO: negative control; BAP: positive control.

CONCLUSION

In summary, six new dihydroisocoumarin derivatives, aspergimarins A−F (**1**−**6**) were obtained along with five known analogs (**7**−**11**) from the fermentation of a fungus *Aspergillus* sp. NBUF87, isolated from the sponge *Hymeniacidon* sp. collected from the Paracel Islands in the South China Sea. Structurally, compounds **2** and **3** are esters of the C-4′ hydroxy group in the C-3 side chain of **1**, representing relatively rare isocoumarin derivatives according to previous literature reports (Saeed, 2016). In a plant growth response assay using *A. thaliana* Col-0 as a model organism, only **1** and **5** showed inhibitory activity against root growth, while the others were inactive at up to 100 μM. This finding indicates that the substitution pattern of hydroxy groups in these dihydroisocoumarins may play an important role in root growth inhibitory activity, and further studies remain necessary to interrogate this phenomenon. Since none of the isolated compounds, including **1** and **5**, were found to be broadly AChE inhibitors, anticancer agents, antibacterial agents, or antimalarial agents, it is proposed that these root growth inhibitors act through more elaborate signaling pathways. Moreover, **1** and **5** were here as the root growth inhibitors of Col-0, suggesting that they have an important impact in agricultural production.

DATA AVAILABILITY STATEMENT

The datasets generated for this study can be found in the Cambridge Structural Database https://www.ccdc.cam.ac.uk/structures/accession1919904.

AUTHOR CONTRIBUTIONS

All authors conceived the research, analyzed the data, contributed to the study, and approved the final version of the manuscript. LH, LD, XL, NW, WC, XW, and JL performed the experiments. LH wrote the manuscript. LD, CN, JL, XY, and SH read and revised the manuscript.

FUNDING

This study was supported by the National Key Research and Development Program of China (2018YFC0310900), the National Natural Science Foundation of China (41776168, 41706167, and 81850410553), Ningbo Public Service Platform for High-Value Utilization of Marine Biological Resources (NBHY-2017-P2), Zhejiang Provincial Public Welfare Technology Program (LGC19B020002), the Natural Science Foundation of Ningbo (2018A610303 and 2018A610320), Ningbo Science and Technology Projects for Common Wealth (2017C10016), the National 111 Project of China (D16013), the Li Dak Sum Yip Yio Chin Kenneth Li Marine Biopharmaceutical Development Fund, and the K. C. Wong Magna Fund in Ningbo University.

SUPPLEMENTARY MATERIAL

The Supplementary Material for this article can be found online at: https://www.frontiersin.org/articles/10.3389/fmicb.2019.02846/full#supplementary-material

REFERENCES

Ahmed, E. F., Rateb, M. E., El-Kassem, L. A., and Hawas, U. W. (2017). Anti-HCV protease of diketopiperazines produced by the Red Sea sponge-associated fungus *Aspergillus versicolor*. *Appl. Biochem. Microbiol.* 53, 101–106. doi: 10.1134/s0003683817010021

Blunt, J. W., Carroll, A. R., Copp, B. R., Davis, R. A., Keyzers, R. A., and Prinsep, M. R. (2018). Marine natural products. *Nat. Prod. Rep.* 35, 8–53. doi: 10.1039/c7np00052a

Cai, R., Wu, Y., Chen, S., Cui, H., Liu, Z., Li, C., et al. (2018). Peniisocoumarins A–J: isocoumarins from *Penicillium commune* QQF-3, an endophytic fungus of the mangrove plant *Kandelia candel*. *J. Nat. Prod.* 81, 1376–1383. doi: 10.1021/acs.jnatprod.7b01018

Chen, H., Xiang, S., Huang, L., Lin, J., Hu, S., Mak, S. H., et al. (2018). Tacrine (10)-hupyridone, a dual-binding acetylcholinesterase inhibitor, potently attenuates scopolamine-induced impairments of cognition in mice. *Metab. Brain Dis.* 33, 1131–1139. doi: 10.1007/s11011-018-0221-7

Chen, Y., Liu, Z., Liu, H., Pan, Y., Li, J., Liu, L., et al. (2018). Dichloroisocoumarins with potential anti-inflammatory activity from the mangrove endophytic fungus *Ascomycota* sp. CYSK-4. *Mar. Drugs* 16, 54–63. doi: 10.3390/md16020054

Chen, M., Wang, R., Zhao, W., Yu, L., Zhang, C., Chang, S., et al. (2019). Isocoumarindole A, a chlorinated isocoumarin and indole alkaloid hybrid metabolite from an endolichenic fungus *Aspergillus* sp. *Org. Lett.* 21, 1530–1533. doi: 10.1021/acs.orglett.9b00385

Chen, S., Liu, Y., Liu, Z., Cai, R., Lu, Y., Huang, X., et al. (2016). Isocoumarins and benzofurans from the mangrove endophytic fungus *Talaromyces amestolkiae* possess α-glucosidase inhibitory and antibacterial activities. *Rsc Adv.* 6, 26412–26420. doi: 10.1039/c6ra02566h

Choukchou-Braham, N., Asakawa, Y., and Lepoittevin, J. P. (1994). Isolation, structure determination and synthesis of new dihydroisocoumarins from *Ginkgo biloba* L. *Tetrahedron Lett.* 35, 3949–3952. doi: 10.1016/s0040-4039(00)76710-4

Ding, L., Li, T., Liao, X., He, S., and Xu, S. (2018). Asperitaconic acids A–C, antibacterial itaconic acid derivatives produced by a marine-derived fungus of the genus *Aspergillus*. *J. Antibiot.* 71, 902–904. doi: 10.1038/s41429-018-0079-2

Elsebai, M. F., and Ghabbour, H. A. (2016). Isocoumarin derivatives from the marine-derived fungus *Phoma* sp. 135. *Tetrahedron Lett.* 57, 354–356. doi: 10.1016/j.tetlet.2015.12.024

Fan, L., Reynolds, D., Liu, M., Stark, M., Kjelleberg, S., Webster, N. S., et al. (2012). Functional equivalence and evolutionary convergence in complex communities of microbial sponge symbionts. *RSC Adv.* 109, E1878–E1887. doi: 10.1073/pnas.1203287109

Gu, B. B., Jiao, F. R., Wu, W., Jiao, W. H., Li, L., Sun, F., et al. (2018). Preussins with inhibition of IL-6 expression from *Aspergillus flocculosus* 16D-1, a fungus isolated from the marine sponge *Phakellia fusca*. *J. Nat. Prod.* 81, 2275–2281. doi: 10.1021/acs.jnatprod.8b00662

Hentschel, U., Usher, K. M., and Taylor, M. W. (2006). Marine sponges as microbial fermenters. *FEMS Microbiol. Ecol.* 55, 167–177. doi: 10.1111/j.1574-6941.2005.00046.x

Huang, L., Ding, L., Li, X., Wang, N., Yan, Y., Yang, M., et al. (2019). A new lateral root growth inhibitor from the sponge-derived fungus *Aspergillus* sp. LS45. *Bioorg. Med. Chem. Lett.* 29, 1593–1596. doi: 10.1016/j.bmcl.2019.04.051

Hussain, H., and Green, I. R. (2017). A patent review of two fruitful decades (1997-2016) of isocoumarin research. *Expert Opin. Ther. Pat.* 27, 1267–1275. doi: 10.1080/13543776.2017.1344220

Kim, D. C., Quang, T. H., Ngan, N. T. T., Yoon, C. S., Sohn, J. H., Yim, J. H., et al. (2015). Dihydroisocoumarin derivatives from marine-derived fungal isolates and their anti-inflammatory effects in lipopolysaccharide-induced BV2 microglia. *J. Nat. Prod.* 78, 2948–2955. doi: 10.1021/acs.jnatprod.5b00614

Kong, F., Zhao, C., Hao, J., Wang, C., Wang, W., Huang, X., et al. (2015). New α-glucosidase inhibitors from a marine sponge-derived fungus, *Aspergillus* sp. OUCMDZ-1583. *RSC Adv.* 5, 68852–68863. doi: 10.1016/j.bmcl.2017.12.049

Lazaro, J. E. H., Nitcheu, J., Mahmoudi, N., Ibana, J. A., Mangalindan, G. C., Black, G. P., et al. (2006). Antimalarial activity of crambescidin 800 and synthetic analogues against liver and blood stage of *Plasmodium* sp. *J. Antibiot.* 59, 583–590. doi: 10.1038/ja.2006.78

Lee, Y. M., Li, J., Zhang, P., Hong, J. K., Lee, C. O., and Jung, J. H. (2011). A cytotoxic fellutamide analogue from the sponge-derived fungus *Aspergillus versicolor*. *B Korean Chem. Soc.* 32, 3817–3820. doi: 10.5012/bkcs.2011.32.10.3817

Lei, H., Lin, X., Han, L., Ma, J., Ma, Q., Zhong, J., et al. (2017). New metabolites and bioactive chlorinated benzophenone derivatives produced by a marine-derived fungus *Pestalotiopsis heterocornis*. *Mar. Drugs* 15, 69–78.

Li, D., Xu, Y., Shao, C. L., Yang, R. Y., Zheng, C. J., Chen, Y. Y., et al. (2012). Antibacterial bisabolane-type sesquiterpenoids from the sponge-derived fungus *Aspergillus* sp. *Mar. Drugs* 10, 234–241. doi: 10.3390/md10010234

Li, S., Wei, M., Chen, G., and Lin, Y. (2012). Two new dihydroisocoumarins from the endophytic fungus *Aspergillus* sp. collected from the south china sea. *Chem. Nat. Compd.* 48, 371–373. doi: 10.1007/s10600-012-0254-9

Li, W., Ding, L., Wang, N., Xu, J., Zhang, W., Zhang, B., et al. (2019). Isolation and characterization of two new metabolites from the sponge-derived fungus *Aspergillus* sp. LS34 by OSMAC approach. *Mar. Drugs* 17, 283–291. doi: 10.3390/md17050283

Li, X., Yang, R., and Chen, H. (2018). The *Arabidopsis thaliana* mediator subunit MED8 regulates plant immunity to *Botrytis Cinerea* through interacting with the basic helix-loop-helix (bHLH) transcription factor FAMA. *PLoS One* 13:e0193458. doi: 10.1371/journal.pone.0193458

Liu, H., Edrada-Ebel, R., Ebel, R., Wang, Y., Schulz, B., Draeger, S., et al. (2009). Drimane sesquiterpenoids from the fungus *Aspergillus ustus* isolated from the marine sponge *Suberites domuncula*. *J. Nat. Prod.* 72, 1585–1588. doi: 10.1021/np900220r

Liu, J. T., Wu, W., Cao, M. J., Yang, F., and Lin, H. W. (2018). Trienic α-pyrone and ochratoxin derivatives from a sponge-derived fungus *Aspergillus ochraceopetaliformis*. *Nat. Prod. Res.* 32, 1791–1797. doi: 10.1080/14786419.2017.1402325

Niu, S., Liu, Q., Xia, J. M., Xie, C. L., Luo, Z. H., Shao, Z., et al. (2018). Polyketides from the deep-sea-derived fungus *Graphostroma* sp. MCCC 3A00421 showed potent antifood allergic activities. *J. Agric. Food Chem.* 66, 1369–1376. doi: 10.1021/acs.jafc.7b04383

Pita, L., Fraune, S., and Hentschel, U. (2016). Emerging sponge models of animal-microbe symbioses. *Front. Microbiol.* 7:2102. doi: 10.3389/fmicb.2016.02102

Qi, J., Shao, C. L., Li, Z. Y., Gan, L. S., Fu, X. M., Bian, W. T., et al. (2013). Isocoumarin derivatives and benzofurans from a sponge-derived *Penicillium* sp. fungus. *J. Nat. Prod.* 76, 571–579. doi: 10.1021/np3007556

Ren, Y., Chao, L. H., Sun, J., Chen, X. N., Yao, H. N., Zhu, Z. X., et al. (2019). Two new polyketides from the fungus *Penicillium oxalicum* MHZ153. *Nat. Prod. Res.* 33, 347–353. doi: 10.1080/14786419.2018.1452001

Saeed, A. (2016). Isocoumarins, miraculous natural products blessed with diverse pharmacological activities. *Eur. J. Med. Chem.* 116, 290–317. doi: 10.1016/j.ejmech.2016.03.025

Santos, W. P., da Silva Carvalho, A. C., dos Santos, Estevam, C., Santana, A. E., and Marçal, R. M. (2012). *In vitro* and *ex vivo* anticholinesterase activities of *erythrina velutina* leaf extracts. *Pharm. Biol.* 50, 919–924. doi: 10.3109/13880209.2011.649429

Sun, J., Zhu, Z. X., Song, Y. L., Ren, Y., Dong, D., Zheng, J., et al. (2017). nti-neuroinflammatory constituents from the fungus *Penicillium purpurogenum* MHZ 111. *Nat. Prod. Res.* 31, 562–567. doi: 10.1080/14786419.2016.1207075

Thomas, T. R. A., Kavlekar, D. P., and LokaBharathi, P. A. (2010). Marine drugs from sponge-microbe association-A review. *Mar. Drugs* 8, 1417–1468. doi: 10.3390/md8041417

Tsukada, M., Fukai, M., Miki, K., Shiraishi, T., Suzuki, T., Nishio, K., et al. (2011). Chemical constituents of a marine fungus, *Arthrinium sacchari*. *J. Nat. Prod.* 74, 1645–1649. doi: 10.1021/np200108h

Wang, W., Liao, Y., Zhang, B., Gao, M., Ke, W., Li, F., et al. (2019). Citrinin monomer and dimer derivatives with antibacterial and cytotoxic activities isolated from the deep sea-derived fungus *Penicillium citrinum* NLG-S01-P1. *Mar. Drugs* 17, 46–54. doi: 10.3390/md17010046

Wang, X., Mou, Y., Hu, J., Wang, N., Zhao, L., Liu, L., et al. (2014). Cytotoxic polyphenols from a sponge-associated fungus *Aspergillus versicolor* Hmp-48. *Chem. Biodivers.* 11, 133–139. doi: 10.1002/cbdv.201300115

Webster, N. S., and Taylor, M. W. (2012). Marine sponges and their microbial symbionts: love and other relationships. *Environ. Microbiol.* 14, 335–346. doi: 10.1111/j.1462-2920.2011.02460.x

Wiese, J., Imhoff, J., Gulder, T., Labes, A., and Schmaljohann, R. (2016). Marine fungi as producers of benzocoumarins, a new class of inhibitors of glycogen-synthase-kinase 3β. *Mar. Drugs* 14, 200–208.

Wu, Y., Chen, S., Liu, H., Huang, X., Liu, Y., Tao, Y., et al. (2019). Cytotoxic isocoumarin derivatives from the mangrove endophytic fungus *Aspergillus* sp. HN15-5D. *Arch. Pharm. Res.* 42, 326–331. doi: 10.1007/s12272-018-1019-1

Zhang, X., Li, Z., and Gao, J. (2018). Chemistry and biology of secondary metabolites from *Aspergillus* Genus. *Nat. Prod. J.* 8, 275–304. doi: 10.2174/2210315508666180501154759

Zhou, Y., Debbab, A., Mándi, A., Wray, V., Schulz, B., Müller, W. E., et al. (2013). Alkaloids from the sponge-associated fungus *Aspergillus* sp. *Eur. J. Org. Chem.* 2013, 894–906.

Zhou, Y., Debbab, A., Wray, V., Lin, W., Schulz, B., Trepos, R., et al. (2014). Marine bacterial inhibitors from the sponge-derived fungus *Aspergillus* sp. *Tetrahedron Lett.* 55, 2789–2792. doi: 10.1080/14786419.2017.1289205

Conflict of Interest: The authors declare that the research was conducted in the absence of any commercial or financial relationships that could be construed as a potential conflict of interest.